ACS Partner Journal

Journal of the American Society for Mass Spectrometry

pubs.acs.org/jasms

Application Note

Ambient Single-Cell Analysis and Native Tissue Imaging Using Laser-Ablation Electrospray Ionization Mass Spectrometry with Increased Spatial Resolution

Michael J. Taylor, Andrey Liyu, Akos Vertes, and Christopher R. Anderton*

Cite This: *J. Am. Soc. Mass Spectrom.* 2021, 32, 2490−2494

Read Online

ACCESS | Metrics & More | Article Recommendations | Supporting Information

ABSTRACT: Laser-ablation electrospray ionization mass spectrometry (LAESI-MS) is an emerging method that has the potential to transform the field of metabolomics. This is in part due to LAESI-MS being an ambient ionization method that requires minimal sample preparation and uses (endogenous) water for *in situ* analysis. This application note details the employment of the "LAESI microscope" source to perform spatially resolved MS analysis of cells and MS imaging (MSI) of tissues at high spatial resolution. This source configuration utilizes a long-working-distance reflective objective that permits both visualization of the sample and a smaller LAESI laser beam profile than conventional LAESI setups. Here, we analyzed 200 single cells of *Allium cepa* (red onion) and imaged *Fittonia argyroneura* (nerve plant) in high spatial resolution using this source coupled to a Fourier transform mass spectrometer for high-mass-resolution and high-mass-accuracy metabolomics.

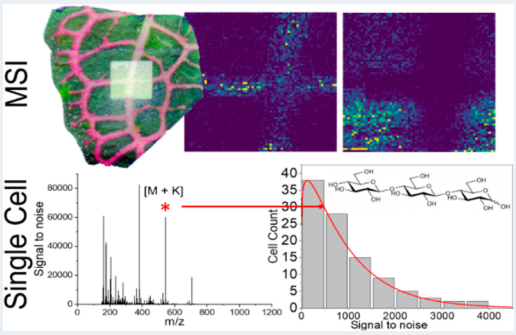

KEYWORDS: *LAESI, native analysis, spatial metabolomics, metabolomics, mass spectrometry imaging*

INTRODUCTION

Mass spectrometry imaging (MSI) is a powerful technique used in spatial metabolomics. MSI methods involve removal via desorption or ablation, ionization, and mass analysis of the metabolic content in a sample in a spatially resolved manner. Typically, an MSI experiment is conducted by preparing the (bio)sample for analysis in a manner that limits sample degradation to ensure high-quality signals and minimizes any spatial delocalization of endogenous species.[1] Analyte delocalization presents a major problem in MSI, which involves changes in the spatial distribution of molecules from their original location within a sample. This can affect the reliability and robustness of MSI measurements. Analyte delocalization can occur from either how the sample is prepared and/or how the sample is analyzed in an MSI experiment. There are multiple studies that detail the main causes of delocalization and its implications.[1−4] However, the degree of delocalization is most pronounced using MSI techniques that require artificial additives to physically support the sample (e.g., embedding) and/or assist in molecule desorption/ionization (e.g., organic matrix coatings) or in methods that require high vacuum for analysis (e.g., secondary ion mass spectrometry). For this reason, there is great interest in MSI approaches that require minimal sample preparation and can be performed under ambient conditions.

Laser-ablation electrospray ionization mass spectrometry (LAESI-MS) (and analogous configurations) can be performed under ambient conditions and requires no sample additives, as it utilizes the native water within tissues for *in situ* metabolomics.[5,6] For this reason, LAESI-MS instruments are increasingly being configured to perform MSI[7] and more recently single-cell metabolomics.[5,8,9] Analysis of single cells using LAESI-MS requires individual cells to be identified and the laser probe to be driven to cell centers sequentially to perform an ablation event.[5,9] Single-cell LAESI-MS is commonly performed using a fiber configuration (f-LAESI), wherein the near-infrared laser is directed through an etched optical fiber, and the fiber tip is driven to cell centroid positions.[10] This approach has been effective for high-spatial- and high-mass-resolution spatial metabolomics in plant systems.[5] However, performing single-cell analysis in high throughput using f-LAESI is challenging, as manual adjustment of the fiber is often required to ablate cells individually, which limits the duty cycle of f-LAESI-MS for single-cell analysis.[5] Instruments that employ an in-line laser-microscope objective offer a benefit over f-LAESI-MS, as they can allow for simultaneous optical microscopy and LAESI-MS of the sample in real time.[11] As such, we have recently demonstrated the

Received: April 27, 2021
Revised: July 19, 2021
Accepted: July 26, 2021
Published: August 10, 2021

potential of our LAESI source with a long-working-distance reflective objective, which can perform said coinciding measurements, for high-throughput single-cell analysis.[11]

Here, we detail high-throughput optically informed single-cell analysis and high-spatial-resolution MSI using our unique dual optical microscope/LAESI source (referred to as the "LAESI microscope"). The first mode enables single-cell LAESI-MS, which we demonstrate by measuring the metabolite content of individual *Allium cepa* cells in a large sample set (n = 200) in high throughput. This was achieved by inputting ~33 optically selected cell positions per tissue sample for automatic analysis with a total duty cycle of ~575 ms per cell. The second mode allows for 40 μm high-spatial-resolution MSI to be conducted without oversampling, which presents a substantial improvement in the performance of LAESI-MS imaging.[5,12] We demonstrated this by imaging *Fittonia argyroneura* leaves, where we were able to identify chemical species specific to the physical structures in the plant leaf. Major sample preparation is eliminated for both sampling modes, and *in situ* spatial metabolomics can be performed on native tissues under ambient sampling conditions. These two analysis modes (targeted single cell and imaging) provide evidence of the potential of this molecular microscope for future spatial metabolomics studies.

EXPERIMENTAL SECTION

Reagents, Chemicals, and Materials. Methanol, water, chloroform, and formic acid were purchased (Fisher Scientific, Hampton, NH, USA) at HPLC grade or higher purity. Agilent Low Concentration Tuning Mix (Agilent Technologies, Santa Clara, CA, USA) was used for mass calibration. Red onion (*A. cepa*) was purchased from a local supermarket, and a nerve plant (*F. argyroneura*) was purchased from a local garden center. ZAP-IT laser alignment paper (Concord, NH, USA) was purchased from zap-it.com.

Instrument Design. The LAESI source component has been described in detail previously, including a precise schematic of the source.[11] Briefly, a CCD camera (Thorlabs Inc., Newton, NJ, USA) is mounted at the top of an optical stack, which records images of the sample placed on a Peltier plate module (Thermo Fisher Scientific, Waltham, MA, USA) on an XYZ stage (Zaber, Vancouver, BC, Canada). A long-working-distance reflective objective (×15, Thorlabs Inc., Newton, NJ, USA) is at the bottom of the optical stack, which allows for simultaneous microscopy and laser ablation. A white light source is directed through a dichroic mirror (long pass, cut-on wavelength, 605 nm, Thorlabs Inc., Newton, NJ, USA) to the sample surface, and the CCD camera records an image. The sample is scanned, and images are recorded at adjacent sample positions. A mid-IR laser source (λ = 2940 nm; OPOTEK, Carlsbad, CA, USA) is directed to the reflective objective through an optical train that contains the dichroic mirror. A continuous electrospray orthogonal to the sample surface intercepts ablated molecules, ionizes, and directs the charged species into the MS inlet. The distance from the sample surface to the MS inlet, ESI tip, and laser objective is sample- and instrument-dependent; however in this study, the distances were recorded as 6.06, 8.01, and 82.58 mm, respectively. For all experiments, a Q-switch delay of 660 μs, a pulse rate of 20 kHz, a power of 1.06 mJ, a fluence of 66 J/cm^2, and 1 laser shot per sample area/cell were used, which was specified in the home-built LabVIEW (2019)-based software.[13] For positive ion mode, the ESI potential was held at 3.5 keV with an ESI spray composition of 0.1% (v/v) formic acid in 1:1 MeOH/water (v/v). For negative ion mode, the ESI potential was held at 3.2 keV with a spray composition of 1:2 (v/v) MeOH/$CHCl_3$. A flow rate of 1.2 μL/min was used in both ionization modes. A Orbitrap Velos Pro hybrid mass spectrometer (Thermo Scientific, Waltham, MA) was used with the mass resolution set to 60K (at 200 m/z), where ions were collected with an accumulation time of 50 ms,[7] and m/z 100−1200 was measured.

Single-Cell Mode. Cell centers are identified manually from optical images acquired from the sample, and a list of cell centroid coordinates are input into a home-built LabVIEW (2019)-based software.[13] Then, the stage moves to each cell center position, and the mid-IR laser source fires upon receiving a trigger pulse from the mass spectrometer followed by moving to the next cell position sequentially, as described before.[11]

Imaging Mode. An image of the sample is acquired using a flatbed slide scanner, and then, the area of the sample intended to be imaged is specified in the home-built LabView software. The step size (40 μm) and number of pixels (in the X and Y directions) are specified in the software. The stage moves to each pixel position and receives a trigger pulse from the mass spectrometer, and a mass spectrum is recorded, followed by moving to the next tile position and repeating the process.[7,11]

***Allium cepa* Single-Cell Analysis.** ZAP-IT paper was used to tune the distance from the objective to the sample surface to optimize the laser focus with respect to spot size. One laser shot was fired over a range of stage heights, the resulting spot diameters were measured, and the ratio of spot width (μm) to spot length (μm) was determined. Square sections of 1 × 1 cm were cut from the outer epidermal layers of a red onion (*A. cepa*) followed by placing of individual sections on a microscope slide. The slide was placed on a precooled Peltier stage (12 °C). Sections were analyzed in triplicate representing a sample set of 100 individual epidermal cells per ionization mode. Spectra were exported as ASCII text files and processed in mMass.[14] Peak picking was performed based on a 2.0 signal-to-noise ratio, and deisotoping was performed. Spectra and histograms with distribution fitting were constructed in OriginPro (2019). Molecular identifications were putatively assigned using METLIN[15] and based on previous work.[11]

***Fittonia argyroneura* High-Spatial-Resolution MSI.** Square sections of 1.5 × 1.5 cm were cut from the center of an *F. argyroneura* leaf, which included regions of the veins and mesophyll. The leaf sections were placed on a microscope slide and then onto the Peltier stage (8 °C) for imaging. The acquisition time per pixel was limited by the scan rate of the Orbitrap. Images were generated as Raw Thermo files and converted into mzML files using proteowizard MS convert,[16] followed by conversion to imzML using the imzML converter.[17] Image files were then uploaded to METASPACE for processing and putative molecular assignments.[18]

RESULTS AND DISCUSSION

Optimizing Laser Focus for Single-Cell Analysis. In order to perform single-cell analysis, the distance from the objective to the sample surface was first optimized to achieve the smallest possible laser spot size (laser spot diameter). The distance from the objective to the sample surface was optimal at 82.58 mm, which resulted in a spot size of 40 μm. An image of the laser spot with dimensions is shown in Figure S1.

https://doi.org/10.1021/jasms.1c00149
J. Am. Soc. Mass Spectrom. 2021, 32, 2490−2494

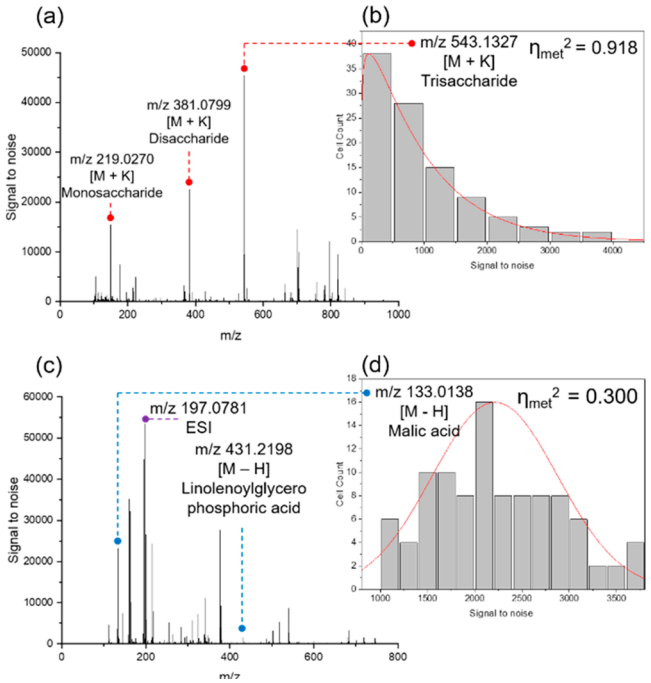

Figure 1. Representative mass spectra (a,c) from a single *Allium cepa* epidermal cell in positive (a) and negative (c) ion mode, with histograms showing trisaccharide (b) and malate (d) variance across a 100-cell data set in each ionization mode.

Single-Cell Analysis of *Allium cepa* Cell Set. Individual cells were ablated, and the metabolite content was measured using our optically directed LAESI microscope coupled to a high-mass-resolution Orbitrap mass spectrometer. Bright-field image pre- and postablation of single *A. cepa* cells can be seen in Figures S2, S3. Spectra from individual single cells are shown in Figure 1a,c with the major identified species shown in Table 1. In positive ion mode (Figure 1a), abundant species include potassiated saccharide adducts of various hexose repeat unit lengths (1−4) at m/z 219.0270, 381.0799, 543.1327, and 705.1856, which we also observed in prior studies of *A. cepa*.[11] The major species observed in negative ion mode (Figure 1c) included malic acid at m/z 133.0138, maleic acid at m/z 115.0032, and mercaptolactic acid at m/z 120.9960. The most abundant ion in negative ion mode can be attributed to the ESI background at m/z 197.0781. Figure 1b,d shows the cell-to-cell variance of two key species represented as histogram plots with their distributions fit across the 100 *A. cepa* cell set. Metabolic noise (η_{met}^2) is also shown for the specific metabolites.[11,19] Metabolic noise is a measure of the metabolite variance across a cell set, and it is calculated by dividing the standard deviation (σ_{met}^2) of the signal/noise for a species across the cell set by the mean abundance (μ_{met}^2). Figure 1b shows that η_{met}^2 = 0.918 for the trisaccharide $[M + K]^+$ detected in positive ion mode with a gamma distribution, whereas Figure 1d shows that η_{met}^2 = 0.300 for malate $[M - H]^-$ in negative ion mode with a Gaussian distribution. The metabolic noise level was observed to exceed the technical noise level measured on our system using verapamil as a technical standard (η_{tech}^2 = 0.003), meaning that these results are biologically significant.

High-Spatial-Resolution 40 μm Imaging of *F. argyroneura*. Our LAESI microscope source also allows for imaging to be conducted by performing a stage scan across tissue-mounted samples. To demonstrate this analysis mode, we

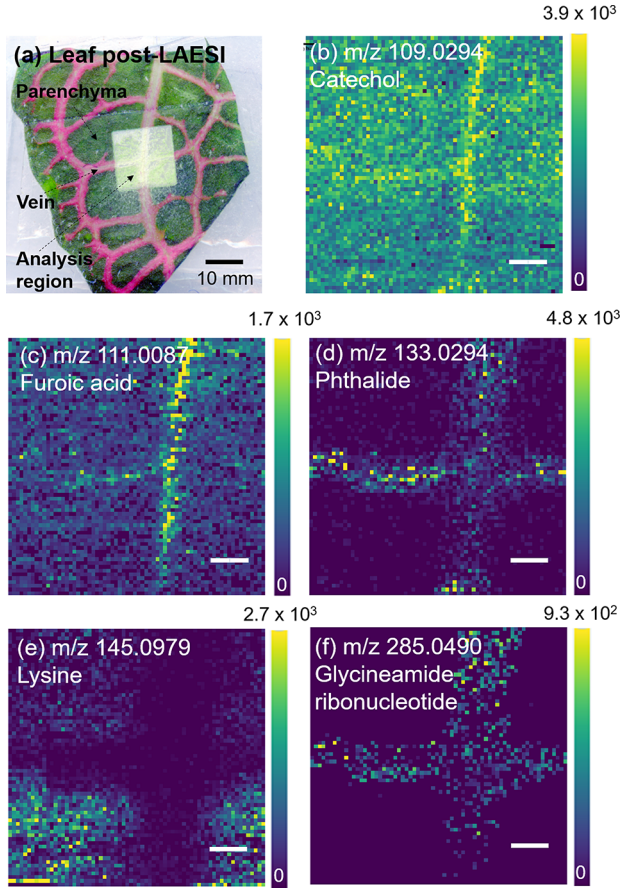

Figure 2. LAESI-MSI of *F. argyroneura* leaf in high spatial resolution (40 μm) in negative ion mode. The total acquisition time was 71 min, and putatively annotated species were identified in METASPACE using the BraChemDB database. The data set is publicly available on METASPACE (https://metaspace2020.eu/project/taylor-2021_). (a) Optical image of leaf post-LAESI imaging showing analysis region (lighter region). Single ion images (b−f): (b) Catechol (vein), (c) furoic acid (vein), (d) phthalide (vein), (e) lysine (parenchyma), (f) glycineamideribonucleotide (vein). Color bars shown as signal/noise, and scale bars are 200 μm.

imaged leaves of *F. argyroneura* (nerve plant; Figures 2 and S4). By adhering the sample to a glass microscope slide using double-sided tape, any differences in sample height when scanning the tissue were minimized. A step size of 40 μm with a beam size of 40 μm, using 1 laser shot per scan, was sufficient to produce metabolite-rich spectra in the absence of any oversampling. From our analysis, numerous species were identified that localized in regions corresponding to physical structures observable in the leaf (Figure 2b−f).

Several putatively annotated species identified in METASPACE are shown in Table 2. The total number of annotated species in METASPACE was recorded at 79 and 371 with a false discovery rate (FDR) of 10 and 20%, respectively, using the BraChemDB database, which demonstrates the spectral richness of this imaging data set. We observed metabolites putatively identified as catechol, furoic acid, phthalide, and glycineamideribonucleotide that localized in the veins of the leaf (Figure 2b−d,f), whereas lysine was detected only in the parenchyma (chloroplast-laden mesophyll; Figure 2e). Furoic acids are a class of secondary metabolites involved in nutrient remobilization; therefore, observing localization of furoic acid in the parenchyma of the leaf may be related to nutrient

https://doi.org/10.1021/jasms.1c00149
J. Am. Soc. Mass Spectrom. 2021, 32, 2490−2494

Table 1. Several Metabolites Identified in Single *A. cepa* Cells[a]

species	structure	observed (m/z)	expected (m/z)	accuracy (ppm)
maleic acid	$[C_4H_4O_4 - H]^-$	115.0032	115.0031	0.8695
malic acid	$[C_4H_6O_5 - H]^-$	133.0138	133.0137	0.7668
mercaptolactic acid	$[C_3H_6O_3S - H]^-$	120.9960	120.9959	0.4959
monosaccharide	$[C_6H_{12}O_6 + K]^+$	219.0273	219.0274	−0.4566
disaccharide	$[C_{12}H_{22}O_6 + K]^+$	381.0801	381.0798	0.7872
trisaccharide	$[C_{18}H_{32}O_{16} + K]^+$	543.1321	543.1320	0.1841
oligosaccharide	$[C_{24}H_{42}O_{21} + K]^+$	689.2109	689.2110	−0.1451

[a]Positive and negatively charged species are included. Putatively annotated species were identified in METLIN.[15]

Table 2. Several Metabolites Identified in *Fittonia argyroneura*[a]

species	structure	observed (m/z)	expected (m/z)	accuracy (ppm)
catechol	$[C_6H_6O_2 - H]^-$	109.0294	109.0293	0.9172
furoic acid	$[C_5H_4O_3 - H]^-$	111.0087	111.0085	1.8020
phthalide	$[C_8H_6O_2 - H]^-$	133.0294	133.0293	0.7517
lysine	$[C_6H_{14}N_2O_2 - H]^-$	145.0979	145.0977	1.3935
monosaccharide	$[C_6H_{12}O_6 + K]^-$	219.0273	219.0274	−0.4565
Gly-rib-ntide	$[C_7H_{15}N_2O_8P - H]^-$	285.0490	285.0488	0.7879
Chr-api-*g*-side	$[C_{27}H_{30}O_{15} - H]^-$	593.1511	593.1506	0.8430

[a]Putatively annotated species were identified in METASPACE using the BraChemDB database.

delivery,[20] whereas the accumulation of lysine within the mesophyll may be related to lysine acetylation of proteins that occurs in the process of photosynthesis within the leaves of plant species.[21] Additionally, we found that these distributions were repeatable across sample replicates, as shown in Figure S4. These results with repeatable distributions demonstrate that LAESI-MS imaging can be used for high-confidence spatial metabolomics of *F. argyroneura*.

CONCLUSION

We have demonstrated that our LAESI-MS microscope allows for both targeted single-cell analysis and MSI. We were able to screen 200 single *A. cepa* cells using this system and perform 40 μm imaging of *F. argyroneura* showing repeatable spatial distribution of metabolites to physical structures within the leaf. The narrow beam profile in our LAESI microscope allows for higher spatial resolution imaging than has reported previously.[22,23] Additionally, this source can be configured to multiple MS detectors as evidenced by prior publications[11] and can be adapted with additional CCD cameras and lens filters for multimodal imaging studies for imaging chromophores.[10] Improvements in optics and ion transmission via ESI containment may further increase the sensitivity of this source. This system therefore has the potential to streamline ambient single-cell analysis and enable high-spatial-resolution LAESI-MS imaging.

ASSOCIATED CONTENT

Supporting Information

The Supporting Information is available free of charge at https://pubs.acs.org/doi/10.1021/jasms.1c00149.

Figure S1: Optical image of ZAP-IT paper showing 40 μm laser spot. Figures S2 and S3: Optical images of *A. cepa* cells pre- and post-LAESI-MS. Figure S4: Optical/2D ion distribution images from *F. argyroneura* secondary data set (PDF)

AUTHOR INFORMATION

Corresponding Author

Christopher R. Anderton − *Earth and Biological Sciences Directorate, Pacific Northwest National Laboratory, Richland, Washington 99352, United States;* orcid.org/0000-0002-6170-1033; Email: christopher.anderton@pnnl.gov

Authors

Michael J. Taylor − *Earth and Biological Sciences Directorate, Pacific Northwest National Laboratory, Richland, Washington 99352, United States;* orcid.org/0000-0001-6926-3720

Andrey Liyu − *Earth and Biological Sciences Directorate, Pacific Northwest National Laboratory, Richland, Washington 99352, United States*

Akos Vertes − *Department of Chemistry, The George Washington University, Washington, D.C. 20052, United States;* orcid.org/0000-0001-5186-5352

Complete contact information is available at: https://pubs.acs.org/10.1021/jasms.1c00149

Author Contributions

M.J.T. and C.R.A. designed all experiments and constructed the LAESI source. M.J.T. performed all experiments and data analysis. A.L. created all the software for the LAESI source. C.R.A. and A.V. conceptualized and designed the source. M.J.T. wrote the paper, and all other authors edited it. All authors have given approval to the final version of the manuscript.

Notes

The authors declare no competing financial interest.

All MSI data sets in this manuscript are publicly available in METASPACE (https://metaspace2020.eu/project/taylor-2021_).

ACKNOWLEDGMENTS

The Authors would like to thank Dr. Sylwia Stopka for helpful discussions. The research was supported by the Intramural

program at EMSL (grid.436923.9), a DOE Office of Science User Facility sponsored by the Biological and Environmental Research program and operated under Contract No. DE-AC05-76RL01830.

REFERENCES

(1) Dong, Y.; Li, B.; Malitsky, S.; Rogachev, I.; Aharoni, A.; Kaftan, F.; Svatoš, A.; Franceschi, P. Sample Preparation for Mass Spectrometry Imaging of Plant Tissues: A Review. *Front. Plant Sci.* **2016**, *7*, 60.

(2) Schaepe, K.; Kokesch-Himmelreich, J.; Rohnke, M.; Wagner, A.-S.; Schaaf, T.; Wenisch, S.; Janek, J. Assessment of Different Sample Preparation Routes for Mass Spectrometric Monitoring and Imaging of Lipids in Bone Cells via ToF-SIMS. *Biointerphases* **2015**, *10* (1), 019016.

(3) Gamble, L. J.; Graham, D. J.; Bluestein, B.; Whitehead, N. P.; Hockenbery, D.; Morrish, F.; Porter, P. ToF-SIMS of Tissues: "Lessons Learned" from Mice and Women. *Biointerphases* **2015**, *10* (1), 019008.

(4) Samarah, L. Z.; Vertes, A. Mass Spectrometry Imaging Based on Laser Desorption Ionization from Inorganic and Nanophotonic Platforms. *View* **2020**, *1* (4), 20200063.

(5) Taylor, M. J.; Lukowski, J. K.; Anderton, C. R. Spatially Resolved Mass Spectrometry at the Single Cell : Recent Innovations in Proteomics and Metabolomics. *J. Am. Soc. Mass Spectrom.* **2021**, *32*, 872.

(6) Bagley, M. C.; Pace, C. L.; Ekelöf, M.; Muddiman, D. C. Infrared Matrix-Assisted Laser Desorption Electrospray Ionization (IR-MALDESI) Mass Spectrometry Imaging Analysis of Endogenous Metabolites in Cherry Tomatoes. *Analyst* **2020**, *145* (16), 5516–5523.

(7) Stopka, S. A.; Samarah, L. Z.; Shaw, J. B.; Liyu, A. V.; Veličković, D.; Agtuca, B. J.; Kukolj, C.; Koppenaal, D. W.; Stacey, G.; Paša-Tolić, L.; Anderton, C. R.; Vertes, A. Ambient Metabolic Profiling and Imaging of Biological Samples with Ultrahigh Molecular Resolution Using Laser Ablation Electrospray Ionization 21 T FTICR Mass Spectrometry. *Anal. Chem.* **2019**, *91* (8), 5028–5035.

(8) Shrestha, B.; Vertes, A. High-Throughput Cell and Tissue Analysis with Enhanced Molecular Coverage by Laser Ablation Electrospray Ionization Mass Spectrometry Using Ion Mobility Separation. *Anal. Chem.* **2014**, *86* (9), 4308–4315.

(9) Samarah, L. Z.; Khattar, R.; Tran, T. H.; Stopka, S. A.; Brantner, C. A.; Parlanti, P.; Veličković, D.; Shaw, J. B.; Agtuca, B. J.; Stacey, G.; Paša-Tolić, L.; Tolić, N.; Anderton, C. R.; Vertes, A. Single-Cell Metabolic Profiling: Metabolite Formulas from Isotopic Fine Structures in Heterogeneous Plant Cell Populations. *Anal. Chem.* **2020**, *92* (10), 7289–7298.

(10) Stolee, J. A.; Shrestha, B.; Mengistu, G.; Vertes, A. Observation of Subcellular Metabolite Gradients in Single Cells by Laser Ablation Electrospray Ionization Mass Spectrometry. *Angew. Chem., Int. Ed.* **2012**, *51* (41), 10386–10389.

(11) Taylor, M. J.; Mattson, S.; Liyu, A.; Stopka, S. A.; Ibrahim, Y. M.; Vertes, A.; Anderton, C. R. Optical Microscopy-Guided Laser Ablation Electrospray Ionization Ion Mobility Mass Spectrometry: Ambient Single Cell Metabolomics with Increased Confidence in Molecular Identification. *Metabolites* **2021**, *11* (4), 200.

(12) Robichaud, G.; Barry, J. A.; Garrard, K. P.; Muddiman, D. C. Infrared Matrix-Assisted Laser Desorption Electrospray Ionization (IR-MALDESI) Imaging Source Coupled to a FT-ICR Mass Spectrometer. *J. Am. Soc. Mass Spectrom.* **2013**, *24* (1), 92–100.

(13) Bitter, R.; Mohiuddin, T.; Nawrocki, M. *LabVIEW: Advanced Programming Techniques*, 2nd ed.; CRC Press, 2006.

(14) Niedermeyer, T. H. J.; Strohalm, M. MMass as a Software Tool for the Annotation of Cyclic Peptide Tandem Mass Spectra. *PLoS One* **2012**, *7* (9), e44913.

(15) Guijas, C.; Montenegro-Burke, J. R.; Domingo-Almenara, X.; Palermo, A.; Warth, B.; Hermann, G.; Koellensperger, G.; Huan, T.; Uritboonthai, W.; Aisporna, A. E.; Wolan, D. W.; Spilker, M. E.; Benton, H. P.; Siuzdak, G. METLIN: A Technology Platform for Identifying Knowns and Unknowns. *Anal. Chem.* **2018**, *90* (5), 3156–3164.

(16) Chambers, M. C.; Maclean, B.; Burke, R.; Amodei, D.; Ruderman, D. L.; Neumann, S.; Gatto, L.; Fischer, B.; Pratt, B.; Egertson, J.; Hoff, K.; Kessner, D.; Tasman, N.; Shulman, N.; Frewen, B.; Baker, T. A.; Brusniak, M.-Y.; Paulse, C.; Creasy, D.; Flashner, L.; Kani, K.; Moulding, C.; Seymour, S. L.; Nuwaysir, L. M.; Lefebvre, B.; Kuhlmann, F.; Roark, J.; Rainer, P.; Detlev, S.; Hemenway, T.; Huhmer, A.; Langridge, J.; Connolly, B.; Chadick, T.; Holly, K.; Eckels, J.; Deutsch, E. W.; Moritz, R. L.; Katz, J. E.; Agus, D. B.; MacCoss, M.; Tabb, D. L.; Mallick, P. A Cross-Platform Toolkit for Mass Spectrometry and Proteomics. *Nat. Biotechnol.* **2012**, *30* (10), 918–920.

(17) Race, A. M.; Styles, I. B.; Bunch, J. Inclusive Sharing of Mass Spectrometry Imaging Data Requires a Converter for All. *J. Proteomics* **2012**, *75* (16), 5111–5112.

(18) Palmer, A.; Phapale, P.; Chernyavsky, I.; Lavigne, R.; Fay, D.; Tarasov, A.; Kovalev, V.; Fuchser, J.; Nikolenko, S.; Pineau, C.; Becker, M.; Alexandrov, T. FDR-Controlled Metabolite Annotation for High-Resolution Imaging Mass Spectrometry. *Nat. Methods* **2017**, *14* (1), 57–60.

(19) Stopka, S. A.; Khattar, R.; Agtuca, B. J.; Anderton, C. R.; Paša-Tolić, L.; Stacey, G.; Vertes, A. Metabolic Noise and Distinct Subpopulations Observed by Single Cell LAESI Mass Spectrometry of Plant Cells in Situ. *Front. Plant Sci.* **2018**, *9*, 1646.

(20) Li, W.; Zhang, H.; Li, X.; Zhang, F.; Liu, C.; Du, Y.; Gao, X.; Zhang, Z.; Zhang, X.; Hou, Z.; Zhou, H.; Sheng, X.; Wang, G.; Guo, Y. Intergrative Metabolomic and Transcriptomic Analyses Unveil Nutrient Remobilization Events in Leaf Senescence of Tobacco. *Sci. Rep.* **2017**, *7* (1), 12126.

(21) Fang, X.; Chen, W.; Zhao, Y.; Ruan, S.; Zhang, H.; Yan, C.; Jin, L.; Cao, L.; Zhu, J.; Ma, H.; Cheng, Z. Global Analysis of Lysine Acetylation in Strawberry Leaves. *Front. Plant Sci.* **2015**, *6*, 739.

(22) Robichaud, G.; Barry, J. A.; Garrard, K. P.; Muddiman, D. C. Infrared Matrix-Assisted Laser Desorption Electrospray Ionization (IR-MALDESI) Imaging Source Coupled to a FT-ICR Mass Spectrometer. *J. Am. Soc. Mass Spectrom.* **2013**, *24* (1), 92–100.

(23) Hieta, J.-P.; Vaikkinen, A.; Auno, S.; Räikkönen, H.; Haapala, M.; Scotti, G.; Kopra, J.; Piepponen, P.; Kauppila, T. J. A Simple Method for Improving the Spatial Resolution in Infrared Laser Ablation Mass Spectrometry Imaging. *J. Am. Soc. Mass Spectrom.* **2017**, *28* (6), 1060–1065.

https://doi.org/10.1021/jasms.1c00149
J. Am. Soc. Mass Spectrom. 2021, 32, 2490–2494

Supplementary information for:

Ambient single cell analysis and native tissue imaging using laser-ablation electrospray ionization mass spectrometry with increased spatial resolution

Michael J. Taylor[1], Andrey Liyu[1], Akos Vertes[2], and Christopher R. Anderton*[1]

[1] Earth and Biological Sciences Directorate, Pacific Northwest National Laboratory, Richland, WA, USA 99352
[2] Department of Chemistry, The George Washington University, Washington, DC 20052

*Christopher.Anderton@pnnl.gov; 902 Battelle Boulevard, Richland, Washington 99352; 509-371-7970

Table of Figures

Figure S1: *Image of ZAP-IT paper showing laser spot size……2*

Figure S2: *Images of Single Allium Cepa Cell pre and post single cell LAESI-MS…….....…2*

Figure S3: *Images of Single Allium Cepa Cell pre and post single cell LAESI-MS …….....3*

Figure S4: *Optical & single ion images of Fittonia argyroneura after 40 μm LAESI-MS imaging…….....3*

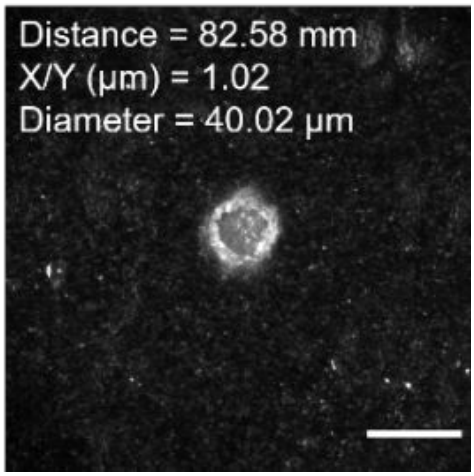

Figure S1. Brightfield image taken of ZAP-IT paper using the optical microscope component of the LAESI microscope source after a single laser shot. Image shows that the IR-laser can be focused to 40 µm for single cell resolution LAESI-MS. Spot size is assessed by the diameter of the crater created in the ZAP-IT paper. The field of view (FOV) for the CCD is 500 x 500 µm. Scale bar (60 µm).

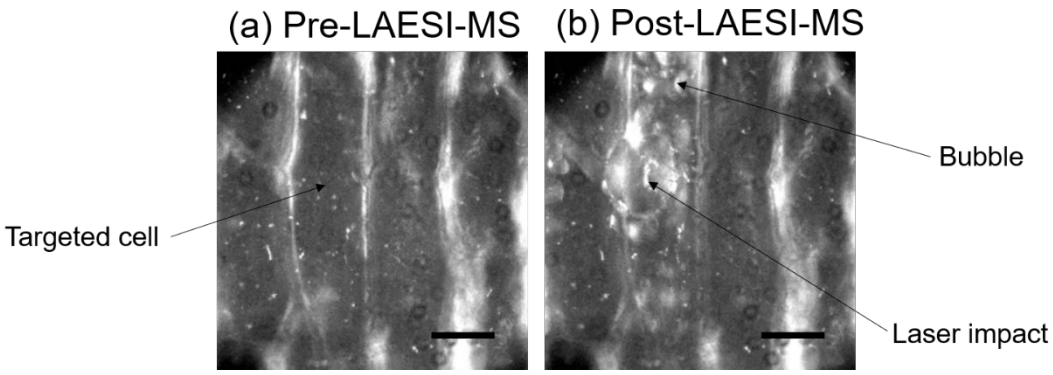

Figure S2. Brightfield images taken of *Allium cepa* epidermal cells using optical train after 1 laser shot. Image shows cell pre (a), and post (b) single cell LAESI-MS, as evidence that single cells can be measured. Scale bars (100 µm).

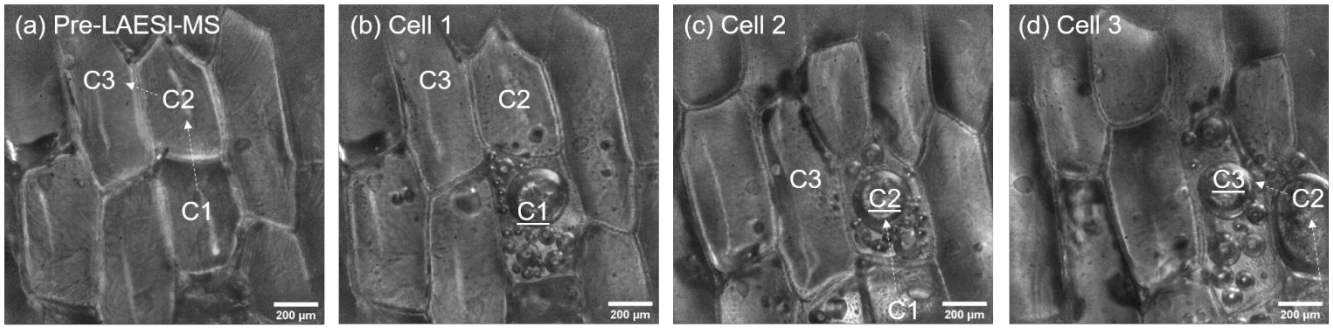

Figure S3. Brightfield images taken of *Allium cepa* epidermal cells using the optical microscopy component of the source pre- and post-LAESI-MS showing individual cells can be targeted and sequentially ablated using optical targeting. (a) Optical image of epidermal cells with cells targeted for LAESI-MS labelled (C1-C3). Optical images of cells post LAESI-MS (b-d).

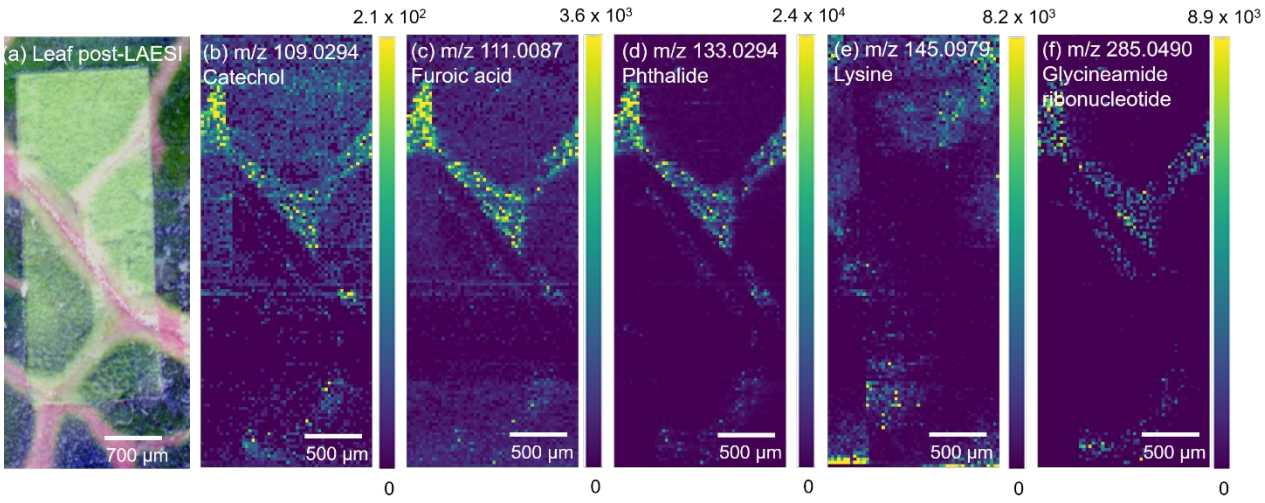

Figure S4. LAESI-MS imaging of *Fittonia argyroneura* (sample 2) using high spatial (40 µm spot size) and high mass resolution mass spectrometry imaging in negative ion mode. The total acquisition time for the image was 140 min. Annotated species were tentatively identified in METASPACE using the BraChemDB database. Dataset is publicly available on METASPACE (https://metaspace2020.eu/project/taylor-2021_) (a) Optical image of leaf post-LAESI-MS imaging showing analysis region (lighter region). Single ion images (b-f). b) Catechol (vein), (c) Furoic acid (vein), (d) Phthalide (vein), (e) Lysine (parenchyma), (f) Glycineamideribonucleotide (vein). Color bars shown as signal/noise.